PHYSICAL REVIEW D **96,** 015024 (2017)

Top quark FCNC couplings at future circular hadron electron colliders

H. Denizli[†] and A. Senol[*]
Department of Physics, Abant Izzet Baysal University, 14280 Bolu, Turkey

A. Yilmaz[‡]
Department of Electric and Electronics Engineering, Giresun University, 28200 Giresun, Turkey

I. Turk Cakir[§] and H. Karadeniz[‖]
Department of Energy Systems Engineering, Giresun University, 28200 Giresun, Turkey

O. Cakir[¶]
Department of Physics, Ankara University, 06100 Ankara, Turkey
(Received 2 May 2017; revised manuscript received 12 June 2017; published 20 July 2017)

A study of single top quark production via flavor changing neutral current interactions at $tq\gamma$ vertices is performed at the future circular hadron electron collider. The signal cross sections for the processes $e^- p \to e^- W^{\pm} q + X$ and $e^- p \to e^- W^{\pm} bq + X$ in the collision of an electron beam with energy $E_e =$ 60 GeV and a proton beam with energy $E_p = 50$ TeV are calculated. In the analysis, the invariant mass distributions of three jets reconstructing top quark mass, requiring one b-tagged jet and two other jets reconstructing the W mass are used to count signal and background events after all selection cuts. The upper limits on the anomalous flavor changing neutral current $tq\gamma$ couplings are found to be $\lambda_q < 0.01$ at the future circular hadron electron collider for $L_{\text{int}} = 100$ fb^{-1} with the fast simulation of detector effects. Signal significance depending on the couplings λ_q is analyzed and an enhanced sensitivity is found to the branching ratio $\text{BR}(t \to q\gamma)$ at the future circular hadron electron collider when compared to the current experimental results.

DOI: 10.1103/PhysRevD.96.015024

I. INTRODUCTION

One of the characteristic features of top quark which makes it very interesting is its large mass. Precise measurements of the couplings among top quark, gauge bosons and quarks are sensitive test of new physics (search for deviations) beyond the standard model (BSM). The cross section for single top quark production via electroweak interactions is about 3 times smaller than the pair production which can be produced by the strong interaction process at the Large Hadron Collider (LHC). Top quark interacts primarily by the strong interaction, but only decays through the weak interaction to a W boson and a bottom quark (most frequently). It provides a unique probe to search for the dynamics of electroweak symmetry breaking. With the high rates, it has the potential for precision studies.

The flavor changing neutral current (FCNC) transitions are not present at the lowest order and suppressed at loop level due to the GIM mechanism in the Standard Model (SM) [1]. Therefore, the top quark FCNC interactions would be a good test of new physics at the present and future colliders. BSM scenarios such as the two-Higgs-doublet model [2], supersymmetry [3], and technicolor [4] predict branching ratios for the top quark FCNC decays of the order of 10^{-6}–10^{-5}. Recent results from the CMS experiment place the upper bound on the top quark FCNC branching ratio from different channels as $\text{BR}(t \to u\gamma) < 1.61 \times 10^{-4}$ and $\text{BR}(t \to c\gamma) < 1.82 \times 10^{-3}$ at 95% confidence level [5].

One of the future collider projects currently under consideration after the LHC era is the Future Circular Collider (FCC) [6] which includes an option for a hadron-electron (FCC-he) collider. This mode is considered to be realized by accelerating electrons up to 60 GeV and colliding them with a beam of protons at the energy of 50 TeV. Recently, the search capability and new physics potential of the FCC-he collider was presented in Ref. [7]. The ep colliders have a broad top physics potential which can be consulted through Refs. [8–18]. Our study is based on the FCC-he which would provide sufficient energy to search for top quark FCNC interactions in a clean environment with suppressed backgrounds from strong interaction process [19,20].

In this work, we investigate the anomalous FCNC $tq\gamma$ couplings via single top quark production for probing the FCNC couplings at the FCC-he collider. In our study, the hadronic decay channel of the W boson in the final state of

[*]Corresponding author.
senol_a@ibu.edu.tr
[†]denizli_h@ibu.edu.tr
[‡]aliyilmaz@giresun.edu.tr
[§]ilkay.turk.cakir@cern.ch
[‖]hande.karadeniz@giresun.edu.tr
[¶]ocakir@science.ankara.edu.tr

the processes $e^- p \to e^- W^{\pm} q + X$ and $e^- p \to e^- W^{\pm} bq + X$ (where q denotes quarks other than top quark) is selected for the signal and background analysis. The event selection and cuts on kinematic variables are discussed in detail. Finally, the discovery potential of anomalous FCNC $tq\gamma$ couplings is examined as a function of luminosity at FCC-he.

II. ANOMALOUS FCNC INTERACTIONS

The higher-order effective operators can be used to describe the BSM effects in model independent way [21]. For the FCNC $tq\gamma$ couplings the effective Lagrangian can be written as [22]

$$L_{\mathrm{FCNC}} = \frac{g_e}{2m_t}\bar{u}\sigma^{\mu\nu}(\lambda^L_{ut}P_L + \lambda^R_{ut}P_R)tA_{\mu\nu} + \frac{g_e}{2m_t}\bar{c}\sigma^{\mu\nu}(\lambda^L_{ct}P_L + \lambda^R_{ct}P_R)tA_{\mu\nu} + \mathrm{H.c.}, \quad (1)$$

where g_e is the electromagnetic coupling constant, $\lambda^{L(R)}_{qt}$ are the strength of anomalous FCNC couplings for $tq\gamma$, which vanish at the lowest order in SM, $P_{L(R)}$ denotes the left-(right-) handed projection operators, and $\sigma^{\mu\nu}$ is the tensor defined as $\sigma^{\mu\nu} = \frac{i}{2}[\gamma^\mu, \gamma^\nu]$ for the FCNC interactions. Here, no specific chirality is assumed for the FCNC interaction vertices, i.e. $\lambda^L_q = \lambda^R_q = \lambda_q$.

The effective Lagrangian can be used to calculate both production cross sections and the branching ratios of the $t \to q\gamma$ decays. At present, the observed bounds on the top quark FCNC decays are still rather weak. However, the low energy flavor transitions mediated by top quark loops may also be affected and could therefore provide helpful information for direct searches at high-energy colliders. The top quark FCNC interactions affect b quark FCNC decays through loop diagrams as mentioned in Ref. [23,24]. The bounds [25] on the real FCNC couplings are lower than the current direct limits but still accessible at the high-luminosity run of LHC. In our calculations, we use the effective interaction vertices at the leading-order level; however, we change its parameters (λ_q) in an accessible range (0–0.05). More vertices with FCNC couplings, each having an order of $\lambda_q \leq 10^{-2}$, contribute less.

III. PRODUCTION CROSS SECTIONS

The existence of the anomalous $tq\gamma$ couplings can lead to the production of a single top quark in ep collisions. The top quark single production processes are sensitive to the top FCNC interactions in the high energy collisions. In this section, to make an estimation for the signal, first we calculate cross section for on-shell single top quark production. The signal cross section for the processes $e^- p \to (e^- t + e^- \bar{t})X$ is given as 3.238×10^{-2} pb while for the process $e^- p \to (e^- t\bar{q} + e^- \bar{t}q)X$ the cross section is 8.106×10^{-3} pb for equal coupling scenario $\lambda_u = \lambda_c = 0.01$ at the center of mass energy $\sqrt{s_{ep}} \simeq 3.46$ TeV of the FCC-he collider. The signal cross sections are given in Table I and Table II for the couplings λ_u and λ_c in the range of (0–0.01). For the cross section calculations, we use `MadGraph5_aMC@NLO` [26] in which the effective FCNC couplings are implemented through the FeynRules package [27] via the Lagrangian described in Eq. (1). We have used the parton distribution function NNPDF23 [28] which is already available within MadGraph 5. In the calculation, we used fixed renormalization and factorization scales at m_Z for the pdf used both in `MadGraph5_aMC@NLO` and Pythia 6 [29]. We obtain the cross section $\sigma_c = 7.58$ fb ($\sigma_u = 24.88$ fb) for the process $e^- p \to (e^- t + e^- \bar{t})X$ and $\sigma_c = 2.96$ fb ($\sigma_u = 5.15$ fb) for the process $e^- p \to (e^- t\bar{q} + e^- \bar{t}q)X$ for couplings $\lambda_u = 0$ and $\lambda_c = 0.01$ ($\lambda_c = 0$ and $\lambda_u = 0.01$), respectively. The cross section depends on λ_u and λ_c with different strengths due to the proton parton distribution function.

TABLE I. The signal cross section values (in pb) for the process $e^- p \to (e^- t + e^- \bar{t})X$ at FCC-he.

FCC-he	$\lambda_c = 10^{-2}$	$\lambda_c = 10^{-3}$	$\lambda_c = 0$
$\lambda_u = 10^{-2}$	3.238×10^{-2}	2.490×10^{-2}	2.488×10^{-2}
$\lambda_u = 10^{-3}$	7.834×10^{-3}	3.243×10^{-4}	2.480×10^{-4}
$\lambda_u = 0$	7.576×10^{-3}	7.580×10^{-5}	0

TABLE II. The signal cross section values (in pb) for the process $e^- p \to (e^- t\bar{q} + e^- \bar{t}q)X$ at FCC-he.

FCC-he	$\lambda_c = 10^{-2}$	$\lambda_c = 10^{-3}$	$\lambda_c = 0$
$\lambda_u = 10^{-2}$	8.106×10^{-3}	5.161×10^{-3}	5.150×10^{-3}
$\lambda_u = 10^{-3}$	3.032×10^{-3}	8.132×10^{-5}	5.142×10^{-5}
$\lambda_u = 0$	2.957×10^{-3}	2.973×10^{-5}	0

IV. SIGNAL AND BACKGROUND ANALYSIS

In this section, the analysis of FCNC $tq\gamma$ couplings through the signal processes $e^- p \to e^- W^{\pm} q + X$ and $e^- p \to e^- W^{\pm} bq + X$, as well as relevant backgrounds at FCC-he, are given. While the first process includes both the signal and the interfering background, the second process includes only the signal. In the analysis, we take into account off-shell top quark FCNC interaction vertices ($tq\gamma$). The Feynman diagrams for the signal processes are shown in Fig. 1. The signal processes are studied through the on-shell W boson production where W boson decays hadronically, and the characterization of the signal processes is given by the presence of at least three jets and an electron in the final state. In order to generate signal and background events, we use `MadGraph5_aMC@NLO` [26]. For the signal, the effective Lagrangian described by Eq. (1) with FCNC couplings is implemented through the FeynRules

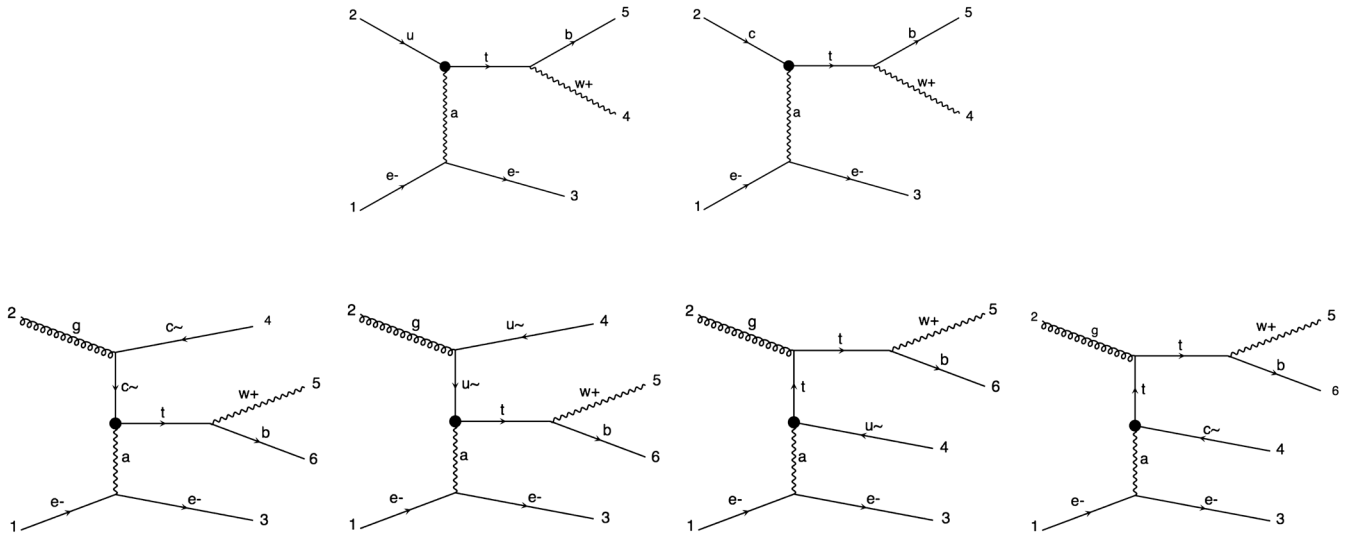

FIG. 1. Feynman diagrams for single top quark production through FCNC vertices and the top quark decays via charged current. The first two diagrams correspond to subprocess $e^- q \to e^- W^+ b$, while the others correspond to $e^- g \to e^- q W^+ b$ which contributes to the signal process.

package [30] into the MadGraph5_aMC@NLO as a universal FeynRules output (UFO) module [27]. PYTHIA 6 and DELPHES 3 [31] are used for parton showering, hadronization, and fast detector simulation, respectively. Jets are clustered using FastJet [32] with the anti-kt algorithm [33], where a cone radius is used as $R = 0.5$. In our analysis, b-tagging with efficiency 75% plays an important role in selecting the final state. The probability of misidentifying the light quark and c quark as a b-jet is taken to be 0.1% and 5%, respectively. In order to distinguish signal and background, we apply the kinematic selection cuts as shown in Table III. At least three jets are required, and an electron is selected in the event with transverse momentum $p_T >$ 20 GeV. The distribution of the number of jets in signal events for $\lambda_q = 0.03$, and also in the most important backgrounds, is given in Fig. 2. One of the three jets is tagged as the b-jet, while the others are used to reconstruct the W boson mass. The b-tagged jet with $p_T > 40$ GeV and two other jets with $p_T > 30$ GeV are considered.

TABLE III. Kinematic cuts used for the analysis of signal and background events. Preselection cuts are used to select the events with three jets and one electron with transverse momentum greater than 20 GeV.

Cuts	Definitions
Cut-0	Preselection cuts with number of jets ≥ 3 and one electron with $p_T^e > 20$ GeV
Cut-1	One jet with b-tagging
Cut-2	$p_T^b > 40$ GeV and $p_T^{j_2,j_3} > 30$ GeV,
Cut-3	$-5 < \eta^{b,j_2,j_3} < 0$ and $-2.5 < \eta^e < 2.5$
Cut-4	60 GeV $< M_{\rm inv}^{\rm rec}(j_2, j_3) <$ 90 GeV
Cut-5	130 GeV $< M_{\rm inv}^{\rm rec}(j_b, j_2, j_3) <$ 200 GeV

Due to the energy asymmetry of the collider, the pseudorapidity of the jets is mainly peaked backward (or forward) of the region depending on the ep (or pe) collisions; therefore, it is taken to be in the interval $-5 < \eta < 0$ for jets and $-2.5 < \eta < 2.5$ for the electron. To reconstruct the W boson from the other two jets, the invariant mass is required to be between 60 and 90 GeV. As a final cut, the reconstructed top quark mass from a b-jet and two other jets is selected to be in the range of 130–200 GeV to count events for further analysis in evaluating the significance for FCNC couplings. After the applied cuts already defined in Table III, the number of signal and all relevant backgrounds is given in Table IV. In Table IV, $S + B_W$ is defined as the signal for both processes

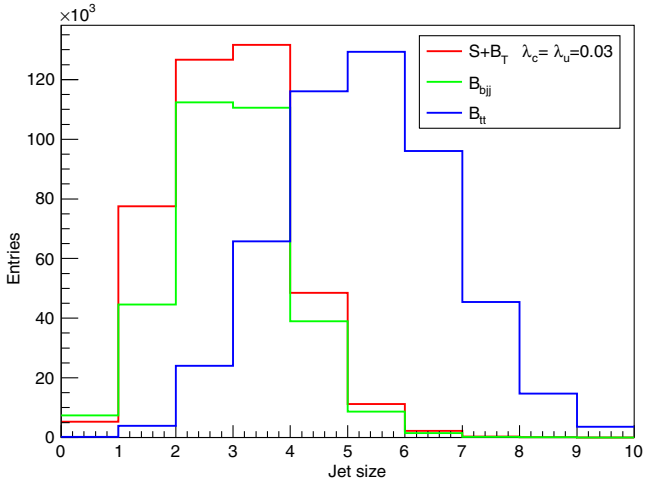

FIG. 2. The distribution of the jet size in signal events and also in the important backgrounds; B_{tt}: $e^- p \to e^- t\bar{t} + X$, B_{bjj}: $e^- q_b \to e^- q_b j_2 + X$, with $q_b = b$ or $\bar{b}$ and $j_2 = q\bar{q}$ or gg.

TABLE IV. The number of signal and relevant background events after each kinematic cuts in the analysis with $L_{\rm int} = 100$ fb^{-1}.

Processes	Cut-0	Cut-1	Cut-2	Cut-3	Cut-4	Cut-5
$S + B_W$ ($\lambda = 0.03$)	206373	11687	8665	7964	2867	1883
$S + B_W$ ($\lambda = 0.01$)	200135	7827	5776	5312	1396	622
S ($\lambda = 0.03$)	6695	4276	3218	2974	1683	1440
S ($\lambda = 0.01$)	457	416	329	322	212	179
B_W	199678	7411	5447	4990	1184	443
B_H	2279	979	802	757	107	47
B_Z	13420	1639	1145	956	246	110
B_{tt}	9752	5594	5339	4974	1079	460
B_{bjj}	48241	17287	9936	9074	2573	1170

and interference background in $e^- p \to e^- W^{\pm} q + X$. Since our signal processes include on-shell W boson and its decay into two jets, we classified the background according to $e + V +$ jets, which includes eWj, eZj, and we also consider the eHj, $ebjj$, and $et\bar{t}$ backgrounds.

The relevant backgrounds are defined as B_W for the process $e^- p \to e^- W^{\pm} q + X$, B_Z for $e^- p \to e^- Z q + X$, B_H for $e^- p \to e^- H q + X$, B_{tt} for $e^- p \to e^- t\bar{t} + X$, B_{bjj} for $e^- q_b \to e^- q_b j_2 + X$ with $q_b = b$ or $\bar{b}$ and $j_2 = q\bar{q}$ or gg. The irreducible SM background B_{bjj} is related to the $2 \to 4$ process which includes both the off-shell W and Z background as well as the $e + 3$ jets backgrounds. The total background will be $B_T \equiv B_{tt} + B_W + B_Z + B_H + B_{bjj}$. The number of events for relevant backgrounds after cut-5 is found to be 1170, 460, 443, 110, and 47 for B_{bjj}, B_{tt}, B_W, B_Z, and B_H, respectively, for the integrated luminosity $L_{\rm int} = 100$ fb^{-1}. For the signal and background (B_W), we obtain 622 events after cut-5 for FCNC coupling $\lambda_q = 0.01$. The major contribution to the background comes from B_{bjj}; only one b-tag is required in the final state. The number of background events depends on the branching into the jets.

Figure 3 shows the distribution of the reconstructed invariant mass of the top quark after cut-4 for different FCNC couplings when both λ_u and λ_c are equal. The left plot shows when both λ equal 0.03 for the signal, and all relevant backgrounds are plotted as well as the ratio $(S + B_W)/B_W$ at the bottom of each one. As can be seen from the ratio plots in Fig. 3, even a small coupling signal is promoted above the total background. According to the inclusion of all relevant backgrounds (B_T), the ratio $[(S + B_T)/B_T)]$ at the top quark mass decreases a factor of about 0.27 for $\lambda = 0.03$ when compared with the respective ratio for B_W.

The statistical significance (SS) is calculated after the final cut by using the Poisson formula,

$$SS = \sqrt{2[(S + B_T)\ln(1 + S/B_T) - S]}, \qquad (2)$$

where S and B_T are the signal and total background events at a particular luminosity. Since the proton beam energy is very large, sensitivity to the λ_u and λ_c couplings is close to each other. The results for the SS values depending on the integrated luminosity (on the left) for the equal coupling scenario are given in Fig. 4. The integrated luminosity versus the FCNC couplings (on the right) at 3σ and 5σ significance is presented in Fig. 4. It is clear from Fig. 4 that even at a luminosity of 35 fb^{-1}, the FCC-he would provide 2σ significance for $\lambda_q = 0.01$, while for an integrated luminosity of 200 fb^{-1}, we obtain 5σ significance at this coupling. With all the relevant backgrounds, we find the 3σ signal significance results to reach an upper limit $\lambda = 0.01$ at the FCC-he with an integrated luminosity of 75 fb^{-1}. One can reach at a lower limit of $\lambda = 0.004$ (0.006) for an observability (discovery) at the integrated luminosity projection of 1 ab^{-1} when it is extrapolated as shown in the right panel of Fig. 4.

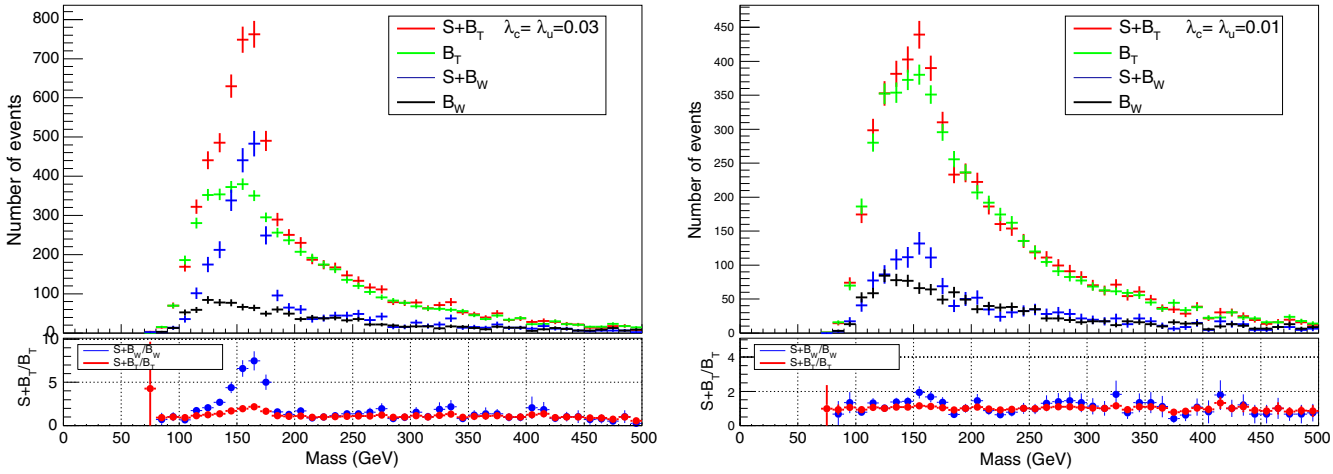

FIG. 3. Distributions of reconstructed invariant mass of top quark plots for signal and relevant backgrounds with different anomalous FCNC couplings. The lower part of each plot shows the relative ratio of $(S + B)$ and B.

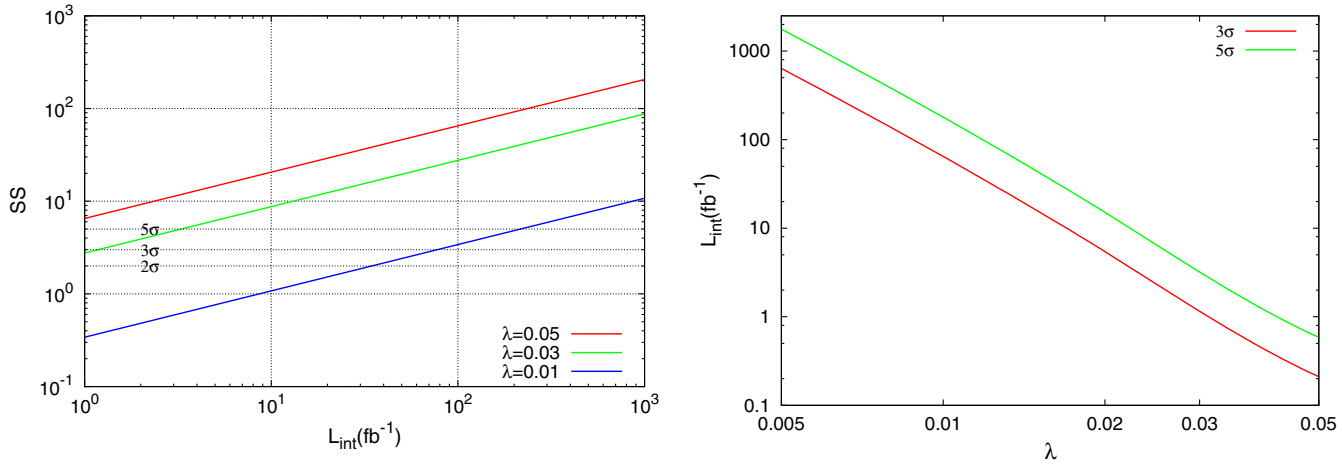

FIG. 4. On the left, the statistical significance depending on integrated luminosity for different anomalous FCNC couplings (λ). On the right, the integrated luminosity versus anomalous FCNC couplings at 3σ and 5σ significance.

There are alternative uses of effective coupling constants appearing in the effective Lagrangian. We express our results in terms of branching ratios which can be comparable with the results of other studies. Using the top quark FCNC decay widths and the total decay width, we can calculate the branching ratio $\mathrm{BR}(t \to q\gamma)$ depending on the coupling λ_q. In order to translate the bounds, the branching ratio is defined as

$$\mathrm{BR}(t \to q\gamma) = \frac{\Gamma(t \to q\gamma)}{\Gamma(t \to q'W^+) + \Gamma(t \to u\gamma) + \Gamma(t \to c\gamma)}. \tag{3}$$

In this equation, we indicate the tree-level prediction for the top quark (t) decay width into a massless down sector quark (q') and a W boson,

$$\Gamma(t \to q'W^+) = \frac{\alpha_e}{16\sin^2\theta_w}|V_{tq'}|^2\frac{m_t^3}{m_W^2}\left[1 - 3\frac{m_W^4}{m_t^4} + 2\frac{m_W^6}{m_t^6}\right]. \tag{4}$$

For the total decay width of the top quark, the main contribution comes from the decay $t \to bW$ with the latest value of about $\Gamma(t \to bW) = 1.41$ GeV [34], because the V_{tb} element of the CKM matrix is much larger than V_{ts} and V_{td}. The partial widths for the FCNC decay channels $t \to q\gamma$ are calculated as $\Gamma(t \to q\gamma) = (1/8)\alpha_e\lambda_q^2 m_t$.

The FCNC coupling $\lambda = 0.004$ can be converted to the branching ratio $\mathrm{BR}(t \to q\gamma) = 2 \times 10^{-6}$ by using Eqs. (3)–(4) and the partial widths for the FCNC decay channels. We obtain smaller branching ratio when compared with previous ep experiments H1 [35] and ZEUS [36] at HERA where they reported limits on the branchings 0.64% and 0.29% at 95% C.L., respectively. At a future ep collider project LHeC [37] planned to run concurrently with the HL-LHC, the upper limits on branching ratios are the order of 10^{-5} for an integrated luminosity of 100 fb^{-1} [38]. Due to the higher energy of the proton beam at FCC-he when compared to the LHeC, it is worth mentioning that the sensitivity to the anomalous $tc\gamma$ coupling will be enhanced compared to the previous limits from ep colliders.

We also compare our results on the branching ratios with the LHC results. Based on proton-proton collisions at 8 TeV within the CMS detector at the LHC at an integrated luminosity of 19.8 fb^{-1}, the limits on the top quark FCNC branching ratios are $\mathrm{BR}(t \to u\gamma) = 1.7 \times 10^{-4}$ and $\mathrm{BR}(t \to c\gamma) = 2.2 \times 10^{-3}$ at 95% C.L. [5]. Our limit on the branching ratio is 1 order smaller than the LHC run-I reach. The projected limits on top FCNC couplings at LHC 14 TeV and HL-LHC have been reported in Ref. [39], where the expected upper limits on branching ratio $t \to q\gamma$ are 8×10^{-5} and 2.5×10^{-5} for an integrated luminosity 300 fb^{-1} and 3000 fb^{-1}, respectively.

V. CONCLUSIONS

We conclude that the FCC-he, with an electron energy of 60 GeV and a proton energy of 50 TeV, would provide significant single top quark production event rates via investigated channel. Top quark FCNC couplings ($\lambda > 0.01$) can be searched at the level of significance greater than 3σ with an integrated luminosity of larger than 75 fb^{-1} at the projected FCC-he. Since b-tagging has an important role for our study, for a more realistic b-tagging efficiency of 60%, statistical significance decreases about 10%, and it also has a similar effect on the limits of couplings. With our analysis for 1 ab^{-1}, the sensitivity to the branching ratio is better than the available experimental limits and comparable or even better then their projected upgrade results.

ACKNOWLEDGMENTS

We acknowledge an exciting discussion within the FCC-he/LHeC Top Physics group. O. Cakir's work was partially supported by Ankara University Scientific Research Projects under Project No. 16L0430018.

[1] S. L. Glashow, J. Iliopoulos, and L.Maiani, Phys. Rev. D **2**, 1285 (1970).
[2] G. Eilam, J. L. Hewett, and A. Soni, Phys. Rev. D **44**, 1473 (1991); **59**, 039901(E) (1998).
[3] J. M. Yang, B. L. Young, and X. Zhang, Phys. Rev. D **58**, 055001 (1998).
[4] G. r. Lu, F. r. Yin, X. l. Wang, and L. d. Wan, Phys. Rev. D **68**, 015002 (2003).
[5] V. Khachatryan *et al.* (The CMS Collaboration), J. High Energy Phys. 04 (2016) 035.
[6] More information is available on the FCC web site: https://fcc.web.cern.ch.
[7] M. Kumar, X. Ruan, R. Islam, A. S. Cornell, M. Klein, U. Klein, and B. Mellado, Phys. Lett. B **764**, 247 (2017).
[8] I. T. Cakir, O. Cakir, and S. Sultansoy, Phys. Lett. B **685**, 170 (2010).
[9] J. Guo, C. X. Yue, J. Zhang, and Q. G. Zeng, Commun. Theor. Phys. **58**, 711 (2012).
[10] I. T. Cakir, A. Senol, and A. T. Tasci, Mod. Phys. Lett. A **29**, 1450021 (2014).
[11] A. O. Bouzas and F. Larios, Phys. Rev. D **88**, 094007 (2013).
[12] L. Xiao-Peng, G. Lei, M. Wen-Gan, Z. Ren-You, H. Liang, and S. Mao, Phys. Rev. D **88**, 014023 (2013).
[13] I. A. Sarmiento-Alvarado, A. O. Bouzas, and F. Larios, J. Phys. G **42**, 085001 (2015).
[14] S. Dutta, A. Goyal, M. Kumar, and B. Mellado, Eur. Phys. J. C **75**, 577 (2015).
[15] A. O. Bouzas and F. Larios, J. Phys. Conf. Ser. **651**, 012004 (2015).
[16] Z. Zhang (LHeC Study Group Collaboration), *Proc. Sci.*, EPS-HEP2015, 342 (2015), arXiv:1511.05399.
[17] W. Liu, H. Sun, X. J. Wang, and X. Luo, Phys. Rev. D **92**, 074015 (2015).
[18] G. R. Boroun, Chin. Phys. C **41**, 013104 (2017).
[19] K. Ohmi and F. Zimmermann, *Proceedings of 6th International Particle Accelerator Conference (IPAC 2015), Richmond, Virginia, USA* (JACoW, 2015).
[20] K. Oide *et al.*, Phys. Rev. Accel. Beams **19**, 111005 (2016).
[21] B. Grzadkowski, M. Iskrzynski, M. Misiak, and J. Rosiek, J. High Energy Phys. 10 (2010) 085.
[22] J. A. Aguilar-Saavedra, Nucl. Phys. **B812**, 181 (2009).
[23] X. Yuan, Y. Hao, and Y. D. Yang, Phys. Rev. D **83**, 013004 (2011).
[24] X. Q. Li, Y. D. Yang, and X. B. Yuan, J. High Energy Phys. 08 (2011) 075.
[25] Y. D. Yang and X. B. Yuan, Chin. Sci. Bull. **59**, 3760 (2014).
[26] J. Alwall, R. Frederix, S. Frixione, V. Hirschi, F. Maltoni, O. Mattelaer, H.-S. Shao, T. Stelzer, P. Torrielli, and M. Zaro, J. High Energy Phys. 07 (2014) 079.
[27] C. Degrande, C. Duhr, B. Fuks, D. Grellscheid, O. Mattelaer, and T. Reiter, Comput. Phys. Commun. **183**, 1201 (2012).
[28] R. D. Ball *et al.*, Nucl. Phys. **B867**, 244 (2013).
[29] T. Sjostrand, S. Mrenna, and P. Z. Skands, J. High Energy Phys. 05 (2006) 026.
[30] A. Alloul, N. D. Christensen, C. Degrande, C. Duhr, and B. Fuks, Comput. Phys. Commun. **185**, 2250 (2014).
[31] J. de Favereau, C. Delaere, P. Demin, A. Giammanco, V. Lemaître, A. Mertens, and M. Selvaggi (DELPHES 3 Collaboration), J. High Energy Phys. 02 (2014) 057.
[32] M. Cacciari, G. P. Salam, and G. Soyez, Eur. Phys. J. C **72**, 1896 (2012).
[33] M. Cacciari, G. P. Salam, and G. Soyez, J. High Energy Phys. 04 (2008) 063.
[34] C. Patriagnani *et al.* (Particle Data Group Collaboration), Chin. Phys. C **40**, 100001 (2016).
[35] F. D. Aaron *et al.* (H1 Collaboration), Phys. Lett. B **678**, 450 (2009).
[36] S. Chekanov *et al.* (ZEUS Collaboration), Phys. Lett. B **559**, 153 (2003).
[37] J. L. Abelleira Fernandez *et al.* (LHeC Study Group Collaboration), J. Phys. G **39**, 075001 (2012).
[38] I. Turk Cakir, A. Yilmaz, H. Denizli, A. Senol, H. Karadeniz, and O. Cakir, arXiv:1705.05419.
[39] ATLAS Collaboration, arXiv:1307.7292.